Journal of The Electrochemical Society, **161** (12) A1860-A1868 (2014)
0013-4651/2014/161(12)/A1860/9/$31.00 © The Electrochemical Society

Characterization of Sulfonated Diels-Alder Poly(phenylene) Membranes for Electrolyte Separators in Vanadium Redox Flow Batteries

Zhijiang Tang,[a] Jamie S. Lawton,[a,*] Che-Nan Sun,[b,*] Jihua Chen,[c,*] Michael I. Bright,[a] Amanda M. Jones,[a] Alex B. Papandrew,[a,*] Cy H. Fujimoto,[d] and Thomas A. Zawodzinski[a,b,e,,z]**

[a]*Department of Chemical and Biomolecular Engineering, University of Tennessee, Knoxville, Tennessee 37996, USA*
[b]*Physical Chemistry of Materials Group, Oak Ridge National Laboratory, Oak Ridge, Tennessee 37831, USA*
[c]*Center for Nanophase Materials Sciences, Oak Ridge National Laboratory, Oak Ridge, Tennessee 37831, USA*
[d]*Organic Materials Science, Sandia National Laboratories, Albuquerque, New Mexico 87185, USA*
[e]*Department of Chemistry, King Abdulaziz University, Jeddah, Saudi Arabia*

Sulfonated Diels-Alder poly(phenylene) (SDAPP) membranes were synthesized and characterized as potential electrolyte separators for vanadium redox flow batteries. The SDAPP membranes studied had ion exchange capacities of 1.4, 1.8 and 2.3 meq/g. Transmission electron microscopy imaging shows that the ionic domains in SDAPP are roughly 0.5 nm in dimension, while Nafion has a hydrophilic phase width of around 5 nm. The sulfuric acid uptake by SDAPP was higher than that for Nafion, but the materials had similar water uptake from solutions of various sulfuric acid concentrations. In equilibration with sulfuric acid concentrations ranging from 0–17.4 mol · kg^{-1}, SDAPP with a IEC of 2.3 meq/g had the highest conductivity, ranging from 0.21 to 0.05 S · cm^{-1}, while SDAPP with a IEC of 1.8 had conductivity close to Nafion 117, ranging from 0.11 to 0.02 S · cm^{-1}. With varying sulfuric acid concentration and temperature, vanadium permeability in SDAPP is positively correlated to the membrane's IEC. The vanadium permeability of SDAPP 2.3 is similar to that of Nafion, but permeability values for SDAPP 1.8 and SDAPP 1.4 are substantially lower. The vanadium permeation decreases with increasing electrolyte sulfuric acid concentration. Vanadium diffusion activation energy is about 20 kJ · mol^{-1} in both SDAPP and Nafion.
 [DOI: 10.1149/2.0631412jes]

Manuscript submitted April 7, 2014; revised manuscript received August 14, 2014. Published September 3, 2014. This was Paper 1697 presented at the San Francisco, California, Meeting of the Society, October 27–November 1, 2013.

The vanadium redox flow battery (VRFB) has shown technical potential for large scale electrical energy storage.[1–3] One possible role of VRFBs is their integration with the electrical grid to "level off" supply and demand mismatches and to improve overall reliability and efficiency of the grid.[1] Another scenario for VRFB use is buffering stochastic energy sources, such as solar or wind, which will improve the stability of electricity output from these renewable resources.[1,4] A VRFB is essentially a regenerative fuel cell, with a flowing operation pattern similar to proton exchange membrane fuel cells.[5,6] In a VRFB the energy is carried by vanadium redox couples V^{5+}/V^{4+} and V^{2+}/V^{3+} in electrolyte solutions. The energy is interconverted between electrical and electrochemical forms by the battery cell or stack, where the functional core is the membrane electrode assembly. The function of the membrane is to separate positive and negative electrolyte solutions and conduct ionic current, while vanadium redox reactions take place on the electrode surface in each half-cell. During battery operation, electrolyte solutions are constantly fed through the battery to support electrochemical reactions and to generate steady current output or recharge the electrolyte solution.

In the VRFB cell, the electrolyte separator is a primary limiting factor in the battery's performance.[3] As has been demonstrated, resistance from the separator is the most important source of the battery's internal resistance, impeding battery performance during high current density operation.[3,7] Ideally, the electrolyte separator should have high conductivity to minimize battery efficiency losses caused by internal resistance and also high ion selectivity to suppress vanadium crossover to maintain battery efficiency and capacity. A commonly used separator for VRFB research is Nafion,[8,9] a perfluorosulfonic acid copolymer cation exchange membrane from DuPont. Unfortunately, due to the high acidity and vanadium concentration in the electrolyte solution, Nafion's conductivity decreases as a result of the electrolyte diffusing into the membrane.[7,10] Capacity loss can also be caused by the rapid vanadium transport across Nafion, which effectively chemically short circuits the cell.[11] The high cost of Nafion is another issue hindering VRFB commercial competiveness, since a low cost electrical storage solution is the only path toward both grid and alternative energy storage commercial success.[12]

Hydrocarbon, aromatic cation exchange membranes are attracting attention from VRFB researchers because their performance is comparable to Nafion in electrochemical devices.[13,14] Aromatic cation exchange membranes are generally developed from thermoplastics by sulfonation which results in high chemical/thermal stability, good mechanical properties and low cost.[15–17] Several hydrocarbon cation exchange membranes have been synthesized and tested in flow batteries; these include sulfonated poly(ether ether ketone) (SPEEK),[16,18] sulfonated poly(phenylsulfone) (S-Radel),[19–21] sulfonated poly(thioether ketone) series (SPTK or SPTKK)[22] and sulfonated Diels-Alder poly(phenylene) (SDAPP).[23]

Sulfonated Diels-Alder poly(phenylene) (SDAPP) was initially synthesized as a proton exchange membrane for PEM fuel cells.[24] SDAPP membranes have been studied as polymer electrolytes for proton exchange membrane fuel cells via investigations of conductivity, permeability and water uptake properties.[25] A preliminary investigation has also been reported on SDAPP as an electrolyte separator in VRFBs.[23] SDAPP membranes can achieve very high ionic selectivity to provide comparable conductivity to Nafion, and also lower VO^{2+} permeability. Membranes with higher IEC had higher ionic conductivity, but lower durability in both long-term battery testing and V^{+5} solutions. We note in passing that that some membranes of this class are not completely stable over the long-term (longer that our typical experiment time!). However, there is an important as yet unmet need to define the physical chemistry of membranes in the context of the environment of a device. Thus, we need to understand membrane behavior for the widest possible range of material types.

In this work, acid and water uptake were examined to determine its impact on the membrane's ionic transport properties relevant to VRFBs. As a reference, Nafion 117 was tested in parallel. The molecular formulas of SDAPP and Nafion are displayed in Figure 1. The sulfuric acid and water uptake properties of SDAPP were quantitatively measured after equilibration in sulfuric acid solutions with concentration ranges between 0 to 17.4 mol · kg^{-1}. After equilibration, the membrane's conductivity was also measured to investigate the influence of the electrolyte-polymer equilibrium on the

*Electrochemical Society Active Member.
**Electrochemical Society Fellow.
zE-mail: tzawodzi@utk.edu

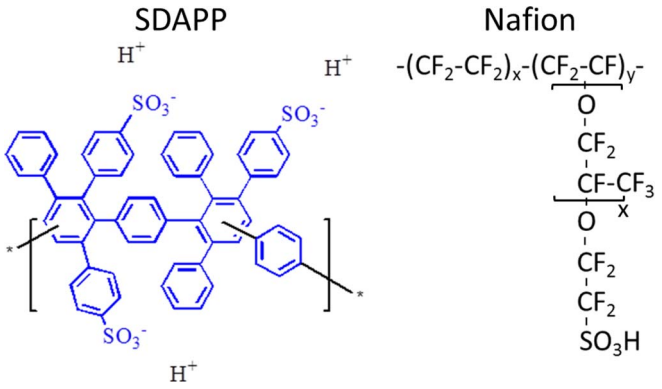

Figure 1. The molecular structures of SDAPP and Nafion. SDAPP is short side chained sulfonated poly(phenylene); Nafion is long sided sulfonated tetrafluoroethylene based copolymer.

membrane's ion transport. Vanadium permeation in SDAPP was measured under different conditions (varying acid concentration or temperature) to study the influence of electrolyte conditions and membrane pore fluid composition on vanadium transport. Transmission electron microscopy work was carried out to study the morphology of SDAPP and ionic domain distribution and size. This work forms the foundation for more detailed studies of ion motion and other chemical details of the interacting membrane and solution.

Experimental

Membrane preparation and characterization.— Sulfonated Diels-Alder poly(phenylene) (SDAPP) membranes with various ion exchange capacities were synthesized as reported previously.[24] The ion exchange capacity (IEC) of the SDAPP polymer was tuned by varying the stoichiometry of the sulfonating agent (chlorosulfuric acid) of Diels-Alder poly(phenylene). The membranes were cast from a solution of 5 wt.% polymer in dimethylacetamide (DMAc) onto a bordered glass plate. After membrane casting and protonation, the membranes were stored in deionized water (Milli Q, 18.0 MΩ · cm) for future characterization and measurement. The ion exchange capacity (IEC) of the SDAPP membranes was determined by the back titration method reported in the literature.[24] Membrane density, ρ, was estimated from membrane weight and dimensions:

$$\rho = \frac{m}{a^2\delta} \quad [1]$$

where m is the measured membrane weight; a is the length of the membrane; and δ is the thickness of the membrane.

Nafion 117 was purchased from Ion Power Inc. and was characterized in parallel for comparison. Before testing, Nafion 117 was sequentially conditioned by in 3% H_2O_2 (Fisher Scientific), DI water, 1 mol · dm^{-3} H_2SO_4 (Alfa Aeser) and DI water for 1 hour at 85°C to remove residual organic and metallic impurities. Pretreated Nafion samples were then kept in DI water until future use.

Transmission electron microscopy.— To study the morphology and sulfonic acid group distribution of the SDAPP membrane, micrographs were taken by transmission electron microscopy. To enhance contrast in images and reveal sulfonic acid distribution, the membrane was exchanged into the Cs^+ form to provide higher electron contrast.[26] SDAPP and Nafion samples were first soaked in 0.1 mol · dm^{-3} Cs_2SO_4 solutions for seven days to reach complete Cs^+ exchange. Then film samples were embedded in a low viscosity epoxy resin (Ted Pella) and microtomed into 70-nm-thick slices. TEM results were collected using a Zeiss Libra 120 at 120 kV with an emission current of 7μA and a minimum dose condition in order to largely mitigate the electron-beam-induced polymer damage. Since standard bright field is used in the microscopy illumination, the hydrophilic phase with sulfonate stained by Cs^+ is dark, while the hydrophobic phase is bright in TEM images.

Acid and water uptake after equilibration in aqueous sulfuric acid.— Sulfuric acid and water uptake in SDAPP and Nafion were measured after equilibration in sulfuric acid solutions of different concentrations. Pretreated acid-form SDAPP and Nafion were first soaked in aqueous sulfuric acid solutions with concentrations ranging from 0 to 17.4 mol · kg^{-1} for 72 hours to reach solution-polymer equilibrium. After equilibration, membrane samples were taken out of solution and their saturated weight was measured as m_{total}. Saturated membrane samples were then boiled in DI water to transfer all imbibed sulfuric acid into the aqueous phase. The sulfuric acid content in water was titrated by a Mettler Toledo DL15 autotitrator with 0.1 mol · dm^{-3} NaOH titrant. Each membrane's dry weight was measured after the boiled membrane was dehydrated in a vacuum oven for 3 hours at 90°C. Water content in membrane after equilibration in sulfuric acid can be calculated by:

$$m_{H_2O} = m_{total} - m_{H_2SO_4} - m_{membrane,dry} \quad [2]$$

The water content in pure water-equilibrated membranes was indexed as the molar ratio of water to sulfonic acid groups in membrane, symbolized as $\lambda = n_{H_2O}/n_{-SO_3H}$.[27]

Membrane conductivity in acidic electrolyte.— To gauge the impact of the membrane's proton conductivity in the presence of sulfuric acid, the membrane samples were equilibrated in sulfuric acid solutions using the same protocol as described previous section. Then, membrane conductivity was measured by electrochemical impedance spectroscopy on a four electrode conductivity cell.[7,24,25] Before measuring, the membrane sample was taken out from the soaking solution, wiped to remove all liquid droplets on the membrane surface and mounted into the conductivity cell. The membrane resistance between two detecting electrodes was equal to the high frequency resistance in the EIS. The high frequency resistance was determined by the intersection of the impedance spectrum with the real impedance axis in the EIS. The membrane's conductivity was calculated from the measured membrane resistance and membrane's corresponding dimensions:

$$\sigma = \frac{L}{R \cdot w \cdot \delta} \quad [3]$$

Here, L is the length between two detecting electrodes; w is the width of membrane samples; δ is membrane thickness. Membrane width and thickness were respectively measured by a Fisherbrand traceable digital calipers and Mitutoyo 543-696 micrometer.

VO^{2+} permeation as a function of sulfuric acid concentration.— To mimic the actual electrolyte in VRFB and understand the role sulfuric acid concentration impacting VO^{2+} permeability across SDAPP membrane, VO^{2+} permeability was measured in the presence of sulfuric acid. VO^{2+} permeability was measured by flowing electrolyte through a 5 cm^2 cross-sectional battery hardware (Fuel Cell Technology) without electrodes through the electron paramagnetic resonance, (EPR) spectrometer cavity. The principle of this measurement has been reported in detail elsewhere.[28,29] During the measurement, VO^{2+} rich solution was placed on one side of the battery, while a receiving solution of the same volume with no VO^{2+} was circulated on the other side of the separator. The volume of the solutions on both sides was 20 mL. The temperature of the cell was stabilized at 30°C by a cartridge heater. The cavity of a Magnettech Miniscope ESR (Berlin, Germany) was built in the tubing line on the receiving side to monitor VO^{2+} accumulation caused by its crossover from the VO^{2+} rich side. The concentration ratio of VO^{2+} and H_2SO_4 in the given solution was controlled at 1:5 and the sulfate concentration on both sides equally ranged from 0.5 to 5 mol · dm^{-3}. The governing equation of mass balance in this diffusion process is:

$$V\frac{dc_r}{dt} = PA\left(\frac{c_g - c_r}{\delta}\right) \quad [4]$$

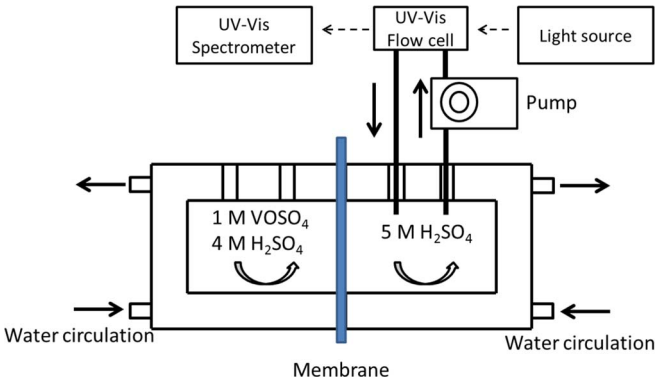

Figure 2. The sketch of VO^{2+} diffusion across membrane monitored by UV-Vis spectrometer with temperature control.

The permeability P can be calculated by:

$$P = -\frac{V\delta}{2At}\ln\left(\frac{c_g^{t=0} - 2c_r^t}{c_g^{t=0}}\right) \quad [5]$$

Where P is the measured membrane permeability; V is the volume of solution on either side of the battery; A is the cross-sectional area of the battery hardware, 5 cm^2; δ is the thickness of the membrane; and t is time the concentration is allowed to equilibrate. Subscripts g and r refers to giving and receiving solutions, respectively.

VO^{2+} permeation as a function of temperature.— VO^{2+} diffusivity in SDAPP was also measured in a Permegear counter diffusion cell at various temperatures, as sketched in Figure 2. On the VO^{2+} rich side of the cell, the solution contains 1 $mol \cdot dm^{-3}$ $VOSO_4$ and 4 $mol \cdot dm^{-3}$ H_2SO_4. On the receiving side, 5 $mol \cdot dm^{-3}$ H_2SO_4 was used to the balance acid strength. The VO^{2+} concentration on the receiving side was monitored by circulating the solution through a UV-Vis flow cell coupled with an ALS-Japan SEC 2000 portable UV-Vis spectrometer. The temperature of the system was conditioned by water circulation in the water jacket of the diffusion cells with a water circulator (Fisher Scientific Isotemp 3016D). During the measurement, the solutions were mixed with magnetic stirrers to minimize the influence of vanadium distribution on the membrane surface. The volume of each cell chamber was 50 mL. The concentration of VO^{2+} in the receiving side can be calculated by Beer-Lambert law. The VO^{2+} mass balance in this measurement also obeys the expression in eq. 4. The diffusivity of VO^{2+} across the membrane can be calculated from eq. 5 as well.

Results and Discussion

Membrane characterization.— The measured ion exchange capacities of synthesized SDAPP membranes were 1.4, 1.8 and 2.3 meq/g. From here on forward, we label the SDAPP membranes as SDAPP 1.4, SDAPP 1.8 and SDAPP 2.3, according to their IEC. Calculated membrane density and water content in the fully hydrated state are presented in Table I, with comparison to Nafion 117.[7] Sulfonic acid group concentration in the membrane under fully hydrated conditions can be calculated by:

$$c_{-SO_3H}^{hydrated} = \frac{EW + 18\lambda}{\rho_{hydrated}} \quad [6]$$

The equivalent weight of the membranes (*EW*), were 714, 555 and 434 grams per mole of sulfonate for SDAPP 1.4, 1.8 and 2.3 respectively. λ is the water content in the pure water equilibrated membrane. $\rho_{hydrated}$ is the membrane density under fully hydrated conditions, calculated from eq. 1. The calculated sulfonic acid concentration in the membranes is presented in Table I. Because SDAPP and Nafion are compositionally variant, (hydrocarbon vs. fluorocarbon) the concentration of sulfonic acid groups can better represent the acid group distribution than IEC. Although SDAPP polymers have significantly higher IEC than Nafion 117, their densities are much lower than Nafion because the SDAPP backbone is formed primarily by C-H bonds while Nafion is composed of heavier C-F bonds. The higher IEC in SDAPP is traded off by the membrane's density, leading to very similar sulfonic acid group concentrations in SDAPPs to those in Nafion, especially for SDAPP 2.3, and Nafion.

Morphology of SDAPP by TEM.— The morphology of the membrane may play a major role in controlling the partitioning or exclusion of ions into the membrane. This is because the energetics of ion uptake are at least partly determined by the charge density in the membrane, which plays a role in the Donnan equilibrium. In comparison with Nafion, SDAPP has a more homogeneous morphology, with less phase separation and a more tortuous structure. The TEM micrographs of SDAPP are presented in Figures 3 and 4, with comparison to Nafion 117 under different magnifications. In these images, dark regions represent hydrophilic domains with Cs^+ stain. Although the state of the film during examination is not equivalent to the conditions of a working flow battery, (specifically regarding the presence of Cs^+ and the fact that the film is dehydrated and held under vacuum), the TEM micrographs can still give us important general information about the microstructure and morphology of the membranes. In

Table I. Density and water content in SDAPP and Nafion membranes at fully hydrated state, and calculated sulfonate concentration.

	SDAPP 1.4	SDAPP 1.8	SDAPP 2.3	Nafion 117[1]
Hydrated density ($g \cdot cm^{-3}$)	1.2	1.2	1.1	1.8
λ	20.4	20.9	24.1	21.6
Sulfonate concentration ($mol \cdot cm^{-3}$)	1.11×10^{-3}	1.27×10^{-3}	1.29×10^{-3}	1.24×10^{-3}

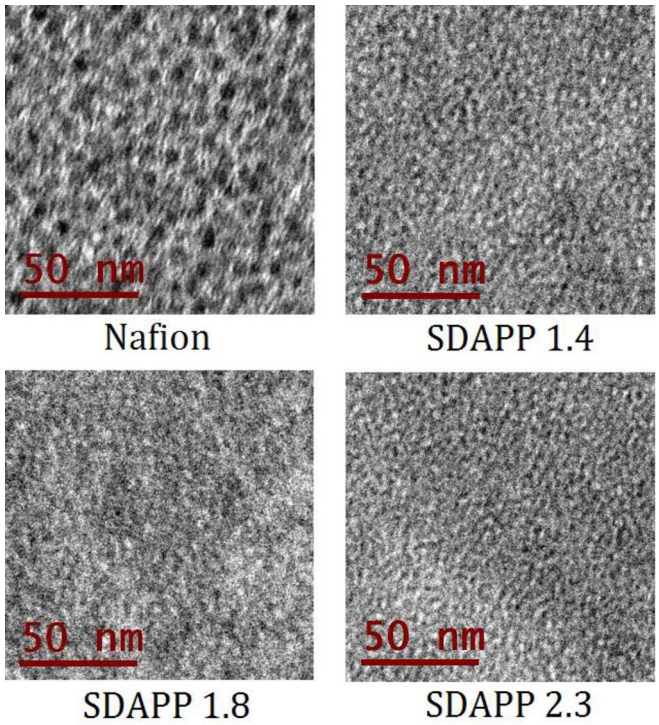

Figure 3. Cs+ stained TEM micrographs of SDAPP and Nafion 117 at 50 nm magnification. More homogeneous sulfonic acid group distribution is presented in SDAPP membranes with varying ion exchange capacity.

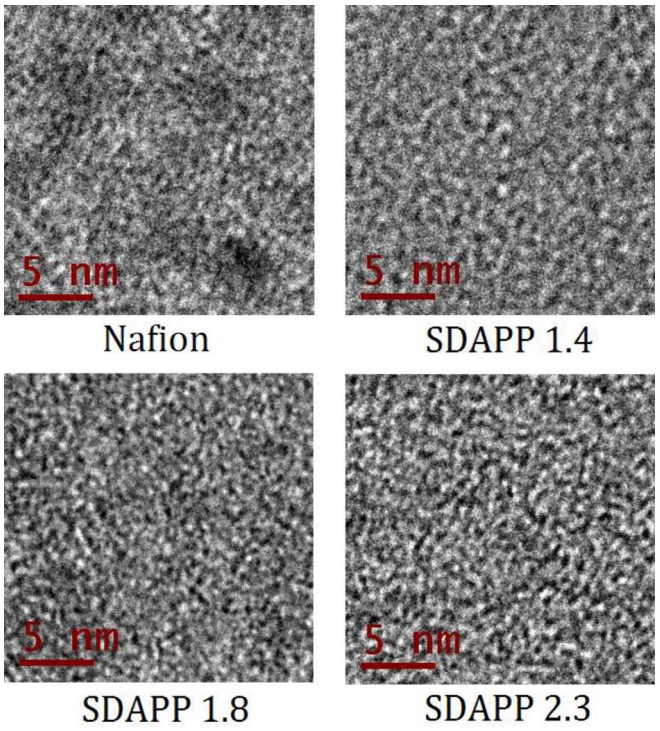

Figure 4. Cs^+ stained TEM micrograph of SDAPP and Nafion 117 at 5 nm magnification. The structure of SDAPP is highly homogeneous and sulfonic acid group is evenly distributed in polymer.

Figure 3, a clear contrast between SDAPP membranes and Nafion 117 in the degree of phase separation is revealed by the TEM imaging at a given magnification. In contrast to the obvious phase separation in Nafion, SDAPP possesses a more homogeneous appearance regardless of its ion exchange capacity. In Nafion the sulfonic acid group can agglomerate and phases separate between the hydrophilic ionic cluster and hydrophobic polymer backbone.[30] The ionic clusters are formed by sulfonate agglomeration and isolated by the hydrophobic polymer matrix, as seen in Figure 3. This feature is consistent with previous studies of PFSA membrane's morphology under dehydrated conditions.[31,32] The length scale of feature width or diameter of hydrophilic and hydrophobic phases is about 5 nm. No well-organized hydrophilic channel network can be observed in the SDAPP polymer in Figure 3.

The size and distribution of the ionic domains in SDAPP membranes are illustrated at a higher magnification in Figure 4. In these images of SDAPP, there are obvious dark and bright areas representing hydrophilic regions and hydrophobic segments of the backbone, respectively. The length scale of the width of hydrophilic and hydrophobic segments in SDAPP is below 1 nm. Considering the C-C distance in benzene is about 0.14 nm,[33] this feature suggests that the sulfonic acid group is not agglomerated but rather is evenly distributed along polymer backbone. The diameter of the ionic cluster in SDAPP is much smaller in size than that in Nafion. Since the ionic cluster is a region surrounded by sulfonic acid groups along polymer backbone, ionic channels of high tortuosity can be developed by the kinked polymer backbone, as can be seen in the micrographs. Tortuous and narrow ionic channels can be observed in all three micrographs of SDAPP membranes, regardless of their IEC. In general, it is likely that the narrow channels in the SDAPP membranes intrinsically hinder transport relative to Nafion. There is likely a trade-off among the water and sulfuric acid content versus this structural factor.

Acid and water uptake after equilibration in various sulfuric acid concentrations.— The sulfuric acid and water contents in SDAPP membranes are presented in Figure 5, with respect to Nafion. Within

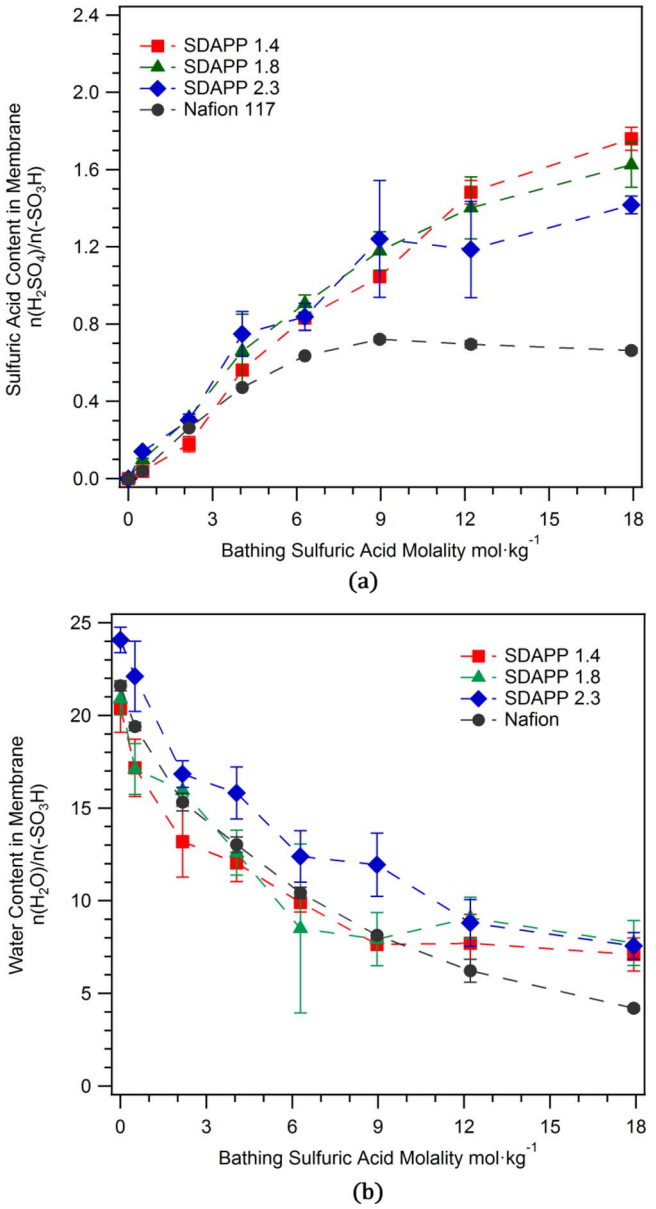

Figure 5. Sulfuric acid (a) and water (b) contents in SDAPP membranes compared to Nafion 117. SDAPP membranes have both significantly higher sulfuric acid and water contents than Nafion in concentrated sulfuric acid environment.

the experimental sulfuric acid concentration range, sulfuric acid can overcome Donnan exclusion from the polymer and enter membrane micropores. Sulfuric acid content in the membrane is characterized as the molar ratio of free sulfuric acid to sulfonic acid groups attached in membrane. As is shown in Figure 5a, the free sulfuric acid contents in SDAPP films with various IECs are similar across the entire sulfuric acid concentration range. This consistency implies that the sulfonic acid group in SDAPP has a uniform ability to exclude or coordinate free anions, regardless of the membrane's IEC. Although the SDAPP membranes have higher ion exchange capacities than Nafion, SDAPP membranes can sorb more sulfuric acid per attached acid than Nafion. This could be a result of weaker Donnan exclusion by the aromatic sulfonic acid groups in SDAPP than by the fluorosulfonic acid group in Nafion. The sulfuric acid content in SDAPP does not level off as seen in Nafion, in which acid content remains constant at 0.7 after 6 mol kg^{-1}. This can be attributed to less 'deswelling' in SDAPP than Nafion in the concentrated sulfuric acid environment. As has been

proven, Nafion loses water substantially, causing reduced internal pore space for imbibed species in low water activity environments.[7,34] Because the sulfonic acid groups in Nafion are attached on a long side chain, it may have a more flexible ionic cluster and channel structure that can deswell significantly in acid solutions.[35] SDAPP has an aromatic backbone with side chains only one benzene ring in length, resulting in a stiff molecular structure to resist deswelling. According to a previous study on mechanical properties of SDAPP membranes, the Young's moduli of SDAPP membranes are substantially higher than those of Nafion, suggesting that the SDAPP membrane has a stronger backbone to resist deswelling caused by acidic solution environments.[24] Accordingly, lower deswelling in SDAPP membranes can allow higher sulfuric acid uptake in the acid concentration range, as is presented in Figure 5.

As shown in Figure 5b, membrane water content is reduced by increasing the bathing sulfuric acid concentration. Since the sulfuric acid in the membrane can be hydrated in addition to the polymer-bound sulfonic acid group, the water content in membrane has to be corrected by incorporating the effects of sulfuric acid. The corrected water content is defined as the molar ratio of water to the total amount of sulfonic acid groups and sulfuric acid, $\lambda' = n_{H_2O}/(n_{-SO_3H} + n_{H_2SO_4})$.[7] The water content in the membranes is independent of IEC or backbone type (hydrocarbon or fluoropolymer). This suggests that the sulfonic acid groups in Nafion and SDAPP have similar hydration properties, not influenced by polymer morphology. The consistent water content also suggests that the sulfuric acid in the membrane's ionic domain might have similar hydration behavior regardless of the sulfonic acid groups in SDAPP or Nafion.

The Donnan exclusion capability of SDAPP is related to the ion exchange capacity of the membrane.[36] The molality of sulfuric acid in the membrane's micropore is presented in Figure 6. The molality of sulfuric acid in the membrane phase is calculated from membrane's sulfuric acid and water content:

$$m_{H_2SO_4} = \frac{n_{H_2SO_4}}{(18\lambda/1000)} \quad [7]$$

The calculated sulfuric acid molality in SDAPP increases with decreasing IEC. The reason for this trend is that at higher IECs, more sulfonic acid groups are present and dissociate into anions and form a stronger potential barrier to exclude sulfuric acid. When comparing SDAPP with aromatic acid groups with fluorosulfonic acid groups in Nafion at equivalent sulfonic concentration (SDAPP 2.3, Nafion; 1.29 $\times 10^{-3}$, 1.24×10^{-3} mol $\cdot$ cm^{-3} respectively in Table I), SDAPP has a higher sulfuric acid molality than Nafion, which suggests that Nafion has a stronger Donnan effect. The different strength of the Donnan exclusion effect in SDAPP and Nafion can be attributed to sulfonic acid group clustering difference in SDAPP and Nafion, besides stronger exclusion from sulfonic acid group in Nafion. Sulfonic acid groups in SDAPP are evenly distributed along the backbone, while sulfonic acid groups in Nafion can agglomerate more effectively.[15,25,35] Since sulfonic acid group concentrations in SDAPP and Nafion are similar, the sulfonate clustering in Nafion can establish a higher *local* potential gradient in the ionic channel to exclude anions. In contrast, the less agglomerated sulfonic acid group in SDAPP generates a lower potential barrier to sulfuric acid than Nafion. The observed differences in Donnan exclusion strength might also be a result of differences in sulfonic acid group acidity. Because the fluorosulfonic acid group in Nafion has a higher acidity than that of the aromatic sulfonic acid group in the hydrocarbon polymer structure of SDAPP,[15] the extent of sulfonic acid group dissociation in SDAPPs would be lower than Nafion, especially at high acid concentration. The less complete sulfonic acid group dissociation and agglomeration in the SDAPPs builds up a weaker potential gradient (compared to Nafion) and reduced Donnan exclusion against co-ions, leading to increase their ability to enter the ionic channel. Discrimination among these possibilities awaits more detailed study and a firmer theoretical grounding.

Sulfuric acid influence on membrane conductivity.— To understand the influence of sulfuric acid concentration on membrane conductivity, all membranes were equilibrated in aqueous sulfuric acid with concentrations that ranged between 0 to 17.4 mol $\cdot$ kg^{-1} (Figure 7). SDAPP 2.3 had the highest conductivity among all three SDAPP membranes, while SDAPP 1.4 has the lowest, which is consistent with the general finding that higher IECs display higher conductivity. Membranes with higher IEC possess higher conductivity because they have more sulfonic acid groups to maintain higher proton concentration for charge transport.[25,37,38] As was shown in Figure 5a, since a considerable amount of sulfuric acid can be present in the membranes, extra protons can be introduced into the membrane to add to the ion conduction. Both SDAPP and Nafion membranes displayed higher conductivity after equilibration in aqueous sulfuric acid, between 0–3 mol $\cdot$ kg^{-1}. However, increasing concentrations of sulfuric acid (>3 mol $\cdot$ kg^{-1}) causes a monotonic decrease in conductivity. This trend is due to the trade-off between increasing proton

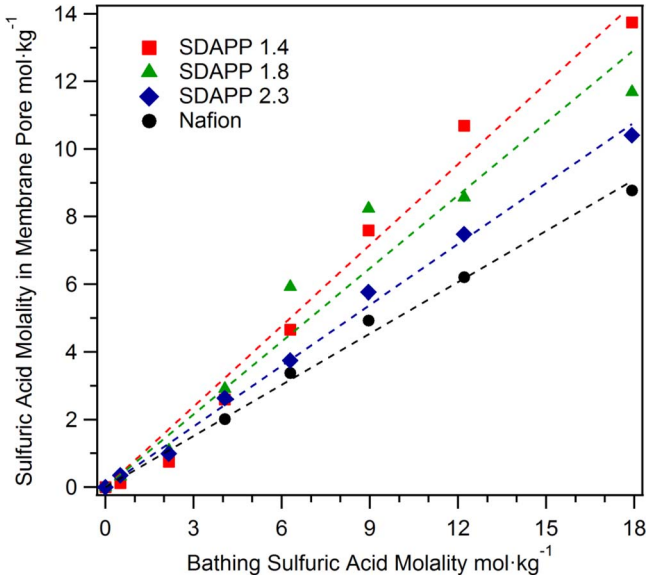

Figure 6. Calculated sulfuric acid molality in membrane phase. Sulfuric acid can be more effectively excluded by Nafion than SDAPP. Donnan exclusion in SDAPP membrane is consistent with membrane ion exchange capacity.

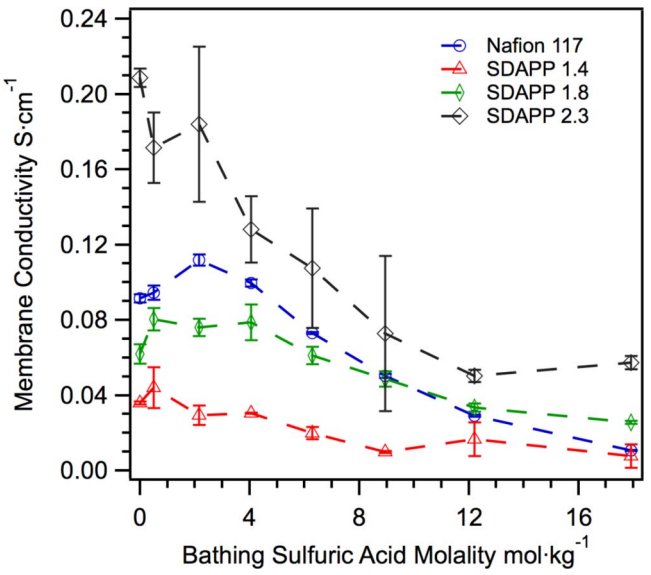

Figure 7. Conductivity of SDAPP membranes after being equilibrated in sulfuric acid solutions with varying concentration. SDAPP membrane with higher IEC has higher conductivity.

concentration in the presence of more acid and proton mobility loss due to reduced water content in the membrane.[7,10]

To analyse proton mobility in the SDAPP membranes, a simple modeling study was carried out based on membrane water uptake and conductivity measurements. The analysis is analogous to the proton transport study on Nafion with sulfuric acid equilibration.[7]

The conductivity of an electrolyte derives from contributions from all mobile charged species in the electrolyte:

$$\sigma = F \sum z_i c_i u_i \qquad [8]$$

Here, F is the Faraday constant, 96500 $C \cdot mol^{-1}$; z_i, c_i and u_i are charge number, ion concentration and mobility of the ion i; the mobile ionic species include proton, bisulfate and sulfate in the SDAPP membranes. Because SDAPP is a cation exchange membrane, anion motion in SDAPP is largely obstructed by the negative electrostatic force from sulfonate in the polymer. It has been proven that anion transference numbers are much lower than protons in cation exchange membrane equilibrated in acids.[10,39] It is therefore rational to approximate that protons are the only charge carrying species in the SDAPP membrane by assuming anion transfer number is negligible. Therefore equation 8 can be simplified to:

$$\sigma = F c_{H^+} u_{H^+} \qquad [9]$$

Proton concentration in the membrane can be calculated from the overall acid (sulfuric acid and sulfonic acid group) concentration in the membrane and acid dissociation. Measured densities of the SDAPP membrane with varying IEC is presented in Table I. Due to the strong acidity of sulfuric acid ($pK_a = -3.0$) and sulfonic acid group ($pK_a = -2.8$ for benzenesulfonic acid),[40] it is assumed that all sulfuric acid and sulfonic acid groups in membrane can completely dissociate into bisulfate or sulfonate, respectively, and an equal amount of protons over the entire sulfuric acid concentration range.[41] It also has been shown that the further dissociation of bisulfate can be fully suppressed by the abundance of protons provided by sulfuric and sulfonic acid groups.[7] Accordingly, the amount of protons in the membrane is equal to the total amount of sulfuric and sulfonic acid groups. Because the sulfuric acid uptake behavior of SDAPP suggests it exhibits a relatively low deswelling effect in sulfuric acid solutions, we assume that the sulfonate concentration in SDAPP does not change substantially when varying the concentration of the sulfuric acid solution. The proton concentration in the membrane then can be calculated by following equation:

$$c_{H^+} = \left(1 + \frac{n_{H_2SO_4}}{n_{-SO_3H}}\right) c_{-SO_3H}^{hydrated} \qquad [10]$$

The calculated proton concentration is presented in Figure 8a. As expected, increasing the concentration of the sulfuric acid bathing solution also increases the proton concentration in the membranes.

Proton mobility in the membrane is then calculated from Equation 8 with membrane conductivity and proton concentration. Although there is an increase in proton concentration in both SDAPP and Nafion membranes with increasing concentration of sulfuric acid in the bathing solution, there is also a decrease in the calculated proton mobility, as is presented in Figure 8b. The bathing sulfuric acid solution influence the membrane conductivity both by raising the membrane proton content and lowering proton mobility. When exposed to a relatively low sulfuric acid concentration, the conductivity enhancement is caused by an increase in proton concentration due to the uptake of sulfuric acid. In more concentrated sulfuric acid solutions, conductivity loss is mainly due to proton mobility loss caused by severe water content loss. The proton concentration in SDAPP is similar to that of Nafion, because the sulfonic acid group and free sulfuric acid concentrations are similar.

Proton mobility in SDAPP is highly favored by increasing the IEC and water content of the membrane. As shown in Figure 9, at any hydration level in the membrane, SDAPP 2.3 has the highest proton mobility followed by SDAPP 1.8 and then SDAPP 1.4. Apparently, proton transport in the SDAPP membrane is favored by a high degree

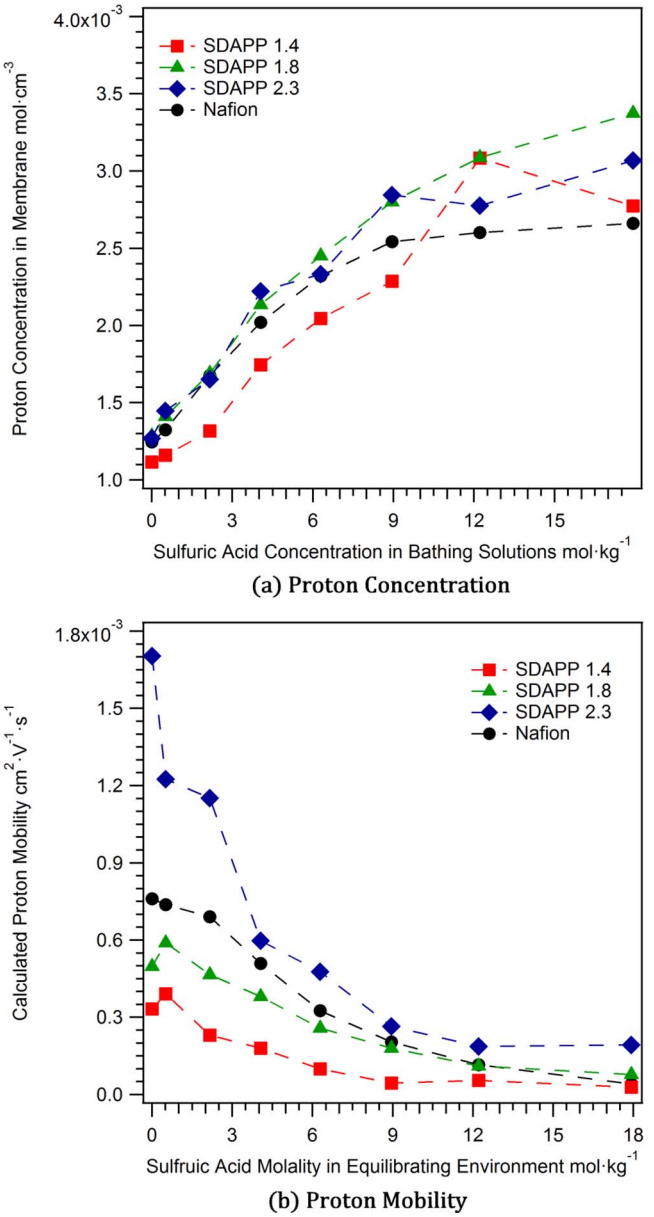

Figure 8. Proton concentration (a) and mobility (b) in SDAPP membranes and Nafion with respect to the sulfuric acid concentration in the bathing environment.

of sulfonation, because higher IEC results in a higher concentration of anionic groups and protons in the ionic domains. As presented in Table I, SDAPP with higher IEC has a higher sulfonate group concentration, so it should also have shorter average inter-sulfonate distance. In addition, it is clear that proton mobility in SDAPP is dependent on water content to an extent similar to Nafion.[27] In hydrated cation exchange membranes, proton transport is favored at high water contents in the membrane because it is facilitated by proton 'hopping' through a well-developed water network via a Grotthuss-type mechanism.[25,27,42] At low water contents, proton transport more relies on a vehicle mechanism, in which proton mobility is highly limited by substantially slower water diffusion.[42]

VO^{2+} transport across SDAPP membranes.— VO^{2+} diffusion rates in SDAPP are consistent with the ion exchange capacity of the membrane: higher IEC results in higher VO^{2+} diffusivity. As shown in Figures 10 and 11, SDAPP 2.3 displays the highest VO^{2+} diffusivity and SDAPP 1.4 has the lowest, regardless of temperature or acid

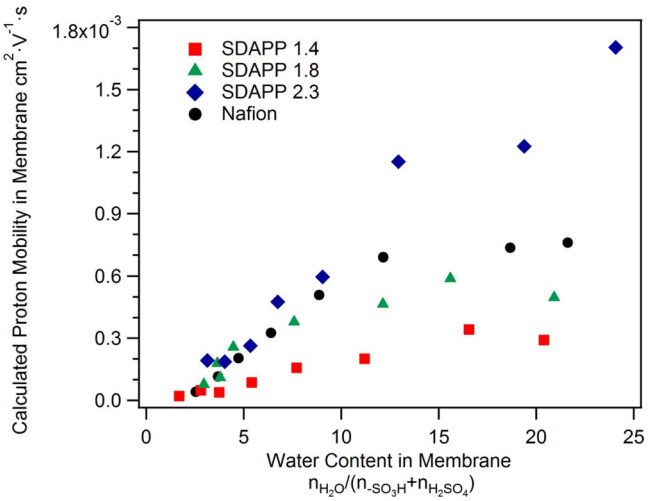

Figure 9. Proton mobility in SDAPP is highly dependent on water content in membrane a. Proton transport in SDAPP is favored by high availability of water molecules to serve as transport intermediator.

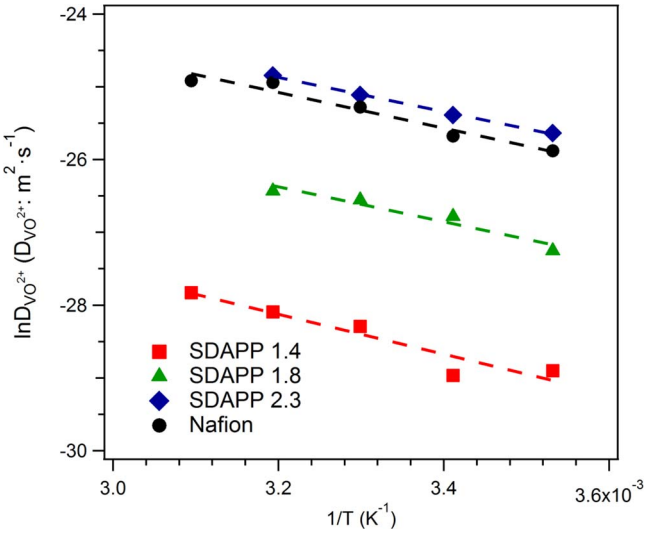

Figure 11. The logarithm of vanadyl diffusivity in SDAPP and Nafion is linearly dependent on 1/T. The vanadyl diffusion in cation exchange membrane obeys classical Arrhenius kinetics.

concentration. Generally, cation diffusivity in cation exchange membranes is consistent with its ion exchange capacity.[18,43] As was just discussed, in membranes with higher IEC, higher amounts of sulfonic acid groups have shorter inter-anion distances to allow higher possibilities for cations to successfully transfer from one sulfonate group to another. Alternatively, the overall membrane porosity and tightness of channels can also affect the transport of ions.

Besides the membrane IEC, vanadium transport is a function of the concentration of acid in the electrolyte solution. As is shown in Figure 10, vanadium permeability across both SDAPP membranes and Nafion is sharply reduced with increasing sulfuric acid concentrations.[29] Figure 5a shows that as the concentration of sulfuric acid in electrolyte increases the amount of sulfuric acid that is absorbed by the membrane also increases. As has been pointed out, the process of cation permeation in the membrane consists of cation partitioning into the polymer and then diffusion through the polymer matrix.[44,45] The process is a competition among cations present. In concentrated electrolyte solutions, the partitioning of VO^{2+} into the membrane is reduced by the presence of sulfuric acid in the membrane.[46] Moreover,

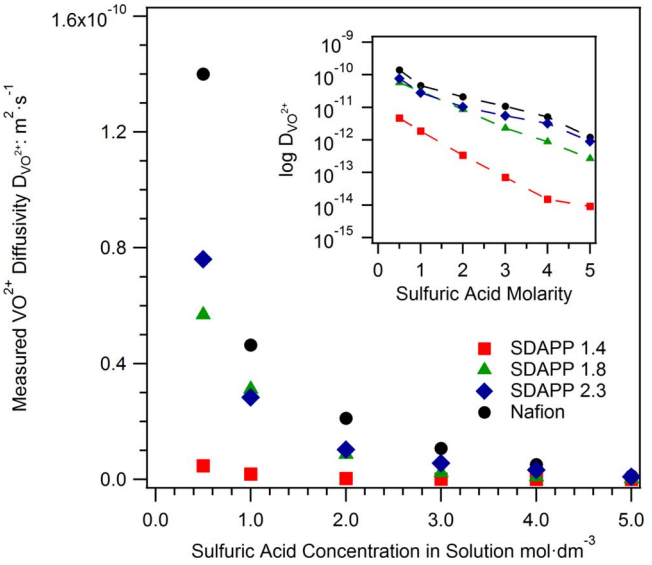

Figure 10. Vanadium permeability across SDAPP membranes is sharply reduced by high sulfuric acid concentration in electrolyte environment.

the dynamics of VO^{2+} transport in the membrane can also be slowed down by the presence of sulfuric acid in membrane.[29] The diffusive medium in the membrane consists of sulfuric acid and water, and the viscosity of the solution increases with sulfuric acid concentration. According to the Stokes-Einstein equation, ionic diffusivity is inversely proportional to the viscosity of diffusion medium, η:

$$D = \frac{k_B T}{6\pi\eta r} \quad [11]$$

Here, k_B is the Boltzmannn constant; r is ionic radius; T is absolute temperature. While VO^{2+} is diffusing within the ionic cluster channel, its motion can be restricted by the viscous friction caused by its interaction with stagnant or slower species in the diffusion media. A higher viscosity of the diffusion medium will result in lower VO^{2+} transport due to a stronger frictional resistance.

VO^{2+} diffusion in SDAPP is also dependent on temperature. According to classical Arrhenius kinetics theory, the diffusivity is dependent on temperature in an exponential form:

$$D = D_0 \exp\left(-E_a/RT\right) \quad [12]$$

In Figure 11, it is shown that the logarithm of VO^{2+} diffusivity is linearly dependent on the reciprocal of temperature in the range between 10 to 50°C. (We note that the range over which we probe temperature dependency is limited by the temperature range of stability of electrolyte solutions with respect to precipitation.) The pre-exponential factors and activation energies for the SDAPP membranes and Nafion are fitted and listed in Table II. The activation energy for VO^{2+} diffusion is fairly similar in all SDAPP membranes and Nafion, regardless of their IEC. This consistency means that VO^{2+} encounters a similar energy barrier for diffusion among sulfonic acid groups in these membranes. The consistent activation energy of VO^{2+} diffusion in the membranes might be due to the similar acidic environment inside the membrane, because they were equilibrated in the same solutions during the diffusivity measurement. In SDAPP membranes, the

Table II. The pre-exponential factor and activation energy for SDAPP membranes and Nafion in Arrhenius kinetics theory.

	SDAPP 1.4	SDAPP 1.8	SDAPP 2.3	Nafion
D_0 (m$^2 \cdot$ s^{-1})	1.49×10^{-9}	7.66×10^{-9}	2.98×10^{-8}	3.24×10^{-8}
E_a (kJ $\cdot$ mol^{-1})	22.8	20.0	19.6	20.3

Table III. Conductivity and VO^{2+} permeability comparison among SDAPPs and Nafion around 20°C. SDAPPs have better conductivity to VO^{2+} permeability ratio than Nafion.

Membrane	SDAPP 1.4	SDAPP 1.8	SDAPP 2.3	Nafion 117
σ $(S \cdot cm^{-1}$ at 22°C)	0.020	0.061	0.107	0.073
$D_{VO^{2+}}$ $(cm^2 \cdot s^{-1}$ at 20°C)	2.64×10^{-9}	2.34×10^{-8}	9.45×10^{-8}	7.07×10^{-8}
$\sigma/\mathbf{D}$ $(S \cdot cm^{-3} \cdot s)$	7.58×10^{6}	2.65×10^{6}	1.13×10^{6}	1.03×10^{6}

activation energy decreases slightly with IEC increase. This means SDAPP membranes with higher IEC has lower energy barrier for VO^{2+} transfer. The activation energy of VO^{2+}, ~20 $kJ \cdot mol^{-1}$, is much higher than that of protons in Nafion, ~10 $kJ \cdot mol^{-1}$.[47] The E_a difference between VO^{2+} and proton suggests that VO^{2+} diffusion across the membrane is much more difficult than proton diffusion.

Here, a detailed investigation has been carried out to quantitatively study SDAPP membranes' ionic transport behavior in vanadium/sulfuric acid electrolyte system. To evaluate the suitability of SDAPP membranes as a VRFB electrolyte separator, compared to commonly-used Nafion, conductivity to vanadyl diffusivity ratios are calculated from measurement results demonstrated above for SDAPPs and Nafion. Uptake data show that all species in the aqueous electrolyte are present in the membrane and are liable to be transported across the membrane. As is presented in Table III, all SDAPP membranes have higher conductivity to vanadyl diffusivity ratios than Nafion in 5M sulfuric acid at about 20°C. This suggests that SDAPP membranes have higher selectivity for proton transport with relative suppression of the unwanted vanadium crossover at given conditions.

Conclusions

In this work, the proton and VO^{2+} transport in sulfonated Diels alder poly(phenylene) membranes with various ion exchange capacities have been studied. The sulfuric acid equilibrium in SDAPP and its impact on SDAPP conductivity were studied based on membrane species content analyses and conductivity tests. SDAPP has higher sulfuric acid uptake than Nafion, likely because it has weaker Donnan exclusion to sulfuric acid than Nafion. Sulfuric acid and sulfonic acid groups in SDAPP have similar hydration to those in Nafion. With a higher ion exchange capacity, SDAPP can achieve comparable conductivity to Nafion 117. At some IECs, SDAPP exhibits a higher ratio of conductivity to vanadium permeability than Nafion. Accordingly SDAPP is a suitable membrane for use as an electrolyte separator for VRFB.

The intrinsically slower ionic transport in SDAPP is most likely due to its homogeneous morphology. Since sulfonic acid groups in SDAPP are attached on short side chains, the short distance between the backbone and acid moiety may not support the agglomeration of sulfonates to and form a hydrophilic phase with a considerable size. The ionic domain in SDAPP is much smaller in radius and is highly tortuous. This structural feature presents larger barriers to transport for the larger VO^{2+} ion than proton because of the stronger ionic interactions with the highly charged vanadyl complex in the smaller ionic channel. The high tortuosity of the membrane is unhelpful for both proton and vanadium transport, because it can reduce the efficiency of ionic diffusion. For future ion exchange membrane development, it is critical to control the size of ionic domains in membrane to enhance ionic selectivity and reduce the tortuosity of ionic channel to improve proton transport. However, the trade-off among these features is subtle.

Acknowledgment

This work is largely supported by the Department of Chemical and Biomolecular Engineering, the University of Tennessee, and Physical Chemistry of Materials Group, Oak Ridge National Laboratory. We gratefully acknowledge the U. S. Department of Energy, Office of Electricity Delivery and Energy Reliability (Dr. Imre Gyuk, Energy Storage Program). Sandia National Laboratories is a multi-program laboratory operated by Sandia Corporation, a wholly owned subsidiary of Lockheed Martin Company, for the U. S. Department of Energy's National Nuclear Security Administration under contract DE-AC04-94AL85000. A portion of this research was conducted at the Center for Nanophase Materials Sciences, which is sponsored at Oak Ridge National Laboratory by the Division of Scientific User Facilities, Office of Basic Energy Sciences, U.S. Department of Energy.

References

1. Z. Yang, J. Zhang, M. C. W. Kintner-Meyer, X. Lu, D. Choi, J. P. Lemmon, and J. Liu, *Chem. Rev.*, **111**, 3577 (2011).
2. A. Z. Weber, M. M. Mench, J. P. Meyers, P. N. Ross, J. T. Gostick, and Q. Liu, *J. Appl. Electrochem.*, **41**, 1137 (2011).
3. R. Zaffou, W. N. Li, and M. L. Perry, in *Polymers for Energy Storage and Delivery Polyelectrolytes for Batteries and Fuel Cells*, p. 107 (2012).
4. L. Joerissen, J. Garche, C. Fabjan, and G. Tomazic, *J. Power Sources*, **127**, 98 (2004).
5. M. Skyllas-Kazacos, M. Rychick, and R. Robins, United States Patent (1988).
6. M. Skyllas-kazacos, D. Kasherman, D. R. Hong, and M. Kazacos, *J. Power Sources*, **35**, 399 (1991).
7. Z. Tang, R. Svoboda, J. S. Lawton, D. S. Aaron, A. B. Papandrew, and T. A. Zawodzinski, *J. Electrochem. Soc.*, **160**, F1040 (2013).
8. S. Kim, E. Thomsen, G. Xia, Z. Nie, J. Bao, K. Recknagle, W. Wang, V. Viswanathan, Q. Luo, X. Wei, A. Crawford, G. Coffey, G. Maupin, and V. Sprenkle, *J. Power Sources*, **237**, 300 (2013).
9. P. Zhao, H. Zhang, H. Zhou, J. Chen, S. Gao, and B. Yi, *J. Power Sources*, **162**, 1416 (2006).
10. G. Pourcelly, A. Lindheimer, C. Gavach, and H. D. Hurwitz, *J. Electroanal. Chem.*, **305**, 97 (1991).
11. C. Sun, J. Chen, H. Zhang, X. Han, and Q. Luo, *J. Power Sources*, **195**, 890 (2010).
12. M. Zhang, M. Moore, J. S. Watson, T. A. Zawodzinski, and R. M. Counce, *J. Electrochem. Soc.*, **159**, A1183 (2012).
13. K. D. Kreuer, in *Handbook of Fuel Cells – Fundamentals, Technology and Applications*, p. 1 (2010).
14. M. Rikukawa and K. Sanui, *Prog. Polym. Sci.*, **25**, 1463 (2000).
15. K. D. Kreuer, *J. Memb. Sci.*, **185**, 29 (2001).
16. P. Xing, G. P. Robertson, M. D. Guiver, S. D. Mikhailenko, K. Wang, and S. Kaliaguine, *J. Memb. Sci.*, **229**, 95 (2004).
17. M. A. Hickner, thesis, Virginia Polytechnic Institute and State Univesity (2003).
18. Z. Mai, H. Zhang, X. Li, C. Bi, and H. Dai, *J. Power Sources*, **196**, 482 (2010).
19. S. Kim, T. B. Tighe, B. Schwenzer, J. Yan, J. Zhang, J. Liu, Z. Yang, and M. A. Hickner, *J. Appl. Electrochem.*, **41**, 1201 (2011).
20. D. Chen, S. Wang, M. Xiao, and Y. Meng, *Energy Convers. Manag.*, **51**, 2816 (2010).
21. S. Kim, J. Yan, B. Schwenzer, J. Zhang, L. Li, J. Liu, Z. Gary, and M. A. Hickner, *Electrochem. Commun.*, **12**, 1650 (2010).
22. D. Chen, S. Wang, M. Xiao, and Y. Meng, *Energy Environ. Sci.*, **3**, 622 (2010).
23. C. Fujimoto, S. Kim, R. Stains, X. Wei, L. Li, and Z. G. Yang, *Electrochem. Commun.*, **20**, 48 (2012).
24. C. H. Fujimoto, M. A. Hickner, C. J. Cornelius, and D. A. Loy, *Macromolecules*, **38**, 5010 (2005).
25. M. A. Hickner, C. H. Fujimoto, and C. J. Cornelius, *Polymer*, **47**, 4238 (2006).
26. S. Rieberer and K. H. Norian, *Ultramicroscopy*, **41**, 225 (1992).
27. T. A. Zawodzinski, C. Derouin, S. Radzinski, R. J. Sherman, V. T. Smith, T. E. Springer, and S. Gottesfeld, *J. Electrochem. Soc.*, **140**, 1041 (1993).
28. J. S. Lawton, D. S. Aaron, Z. Tang, and T. A. Zawodzinski, *J. Memb. Sci.*, **428**, 38 (2013).
29. J. S. Lawton, A. Jones, and T. Zawodzinski, *J. Electrochem. Soc.*, **160**, A697 (2013).
30. W. Y. Hsu and T. D. Gierke, *J. Memb. Sci.*, **13**, 307 (1983).
31. G. Gebel, *Polymer*, **41**, 5829 (2000).
32. A. Z. Weber and J. Newman, *J. Electrochem. Soc.*, **150**, A1008 (2003).
33. K. Tamagawa, T. Iijima, and M. Kimura, *J. Mol. Struct.*, **30**, 243 (1976).
34. M. W. Verbrugge and R. F. Hill, *J. Phys. Chem.*, **92**, 6778 (1988).
35. K. A. Mauritz and R. B. Moore, *Chem. Rev.*, **104**, 4535 (2004).
36. F. Helfferich, in *Ion Exchange*, p. 162, McGraw-Hill, New York (1962).
37. J. J. Fontanella, C. A. Edmondson, M. C. Wintersgill, Y. Wu, and S. G. Greenbaum, *Macromolecular*, **29**, 4944 (1996).

38. S. J. Hamrock and M. A. Yandrasits, *J. Macromol. Sci. Part C Polym. Rev.*, **46**, 219 (2006).
39. G. G. Pourcelly, A. A. Lindheimer, G. Pamboutzoglou, and C. Gavach, *J. Electroanal. Chem.*, **259**, 113 (1989).
40. J. P. Guthrie, *Can. J. Chem.*, **56**, 2342 (1978).
41. G. E. Walrafen and D. M. Dodd, *Trans. Faraday Soc.*, **57**, 1286 (1961).
42. M. A. Hickner, *J. Polym. Sci. Part B Polym. Phys.*, **50**, 9 (2012).
43. X. Luo, Z. Lu, J. Xi, Z. Wu, W. Zhu, and L. Chen, *J. Phys. Chem. B*, **109**, 20310 (2005).
44. J. Crank, *The Mathemaitcs of Diffusion*, Oxford University Press, New York (1977).
45. J. Tong and J. L. Anderson, *Biophys. J.*, **70**, 1505 (1996).
46. Z. Tang, M. Bright, and T. A. Zawodzinski, in *223rd ECS Meeting* (2013).
47. P. Costamagna, C. Yang, A. B. Bocarsly, and S. Srinivasan, *Electrochim. Acta*, **47**, 1023 (2002).